

## CONTROL OF THE POROUS STRUCTURE OF CELLULOSE-BASED TISSUE ENGINEERING SCAFFOLDS BY MEANS OF LYOPHILIZATION

ODETA PETRAUSKAITE,\* GINTARAS JUODZBALYS,\*\* PRANAS VISKELIS\*\*\* and JOLANTA LIESIENE\*

\* *Department of Polymer Chemistry and Technology, Kaunas University of Technology, 19, Radvilenu Pl., LT-50254 Kaunas, Lithuania*

\*\* *Department of Oral and Maxillofacial Surgery, Lithuanian University of Health Sciences, 2, Eiveniu Str., LT-50009 Kaunas, Lithuania*

\*\*\* *Institute of Horticulture, Lithuanian Research Centre for Agriculture and Forestry, 30, Kaunas Str. LT-54333 Babtai, Lithuania*

✉ *Corresponding author: Jolanta Liesiene, jolanta.liesiene@ktu.lt*

Received May 6, 2014

The porous structure of tissue engineering scaffolds that serve as templates for bone tissue regeneration must be precisely designed as it is related to cell adhesion, proliferation, differentiation and vascularization. In this work, the morphology of a three-dimensional matrix of regenerated cellulose prepared by the freeze-drying method was studied. The regenerated cellulose-based gel was obtained by saponification of cellulose acetate. Lyophilization was chosen to create a highly porous matrix with an optimal pore size required for successful bone regeneration. It was found that the porous structure of the gel depended on the solution in its discontinuous phase prior to the drying process. By changing the concentration of ethanol in the discontinuous phase, the morphology of the lyophilized matrix varied from macroporous to dense. The matrix of the desired morphology with micro and macro pores was obtained by lyophilization of the gel, which was filled with 20% of ethanol solution in water and pre-frozen at -25°C. The cellulose based matrix showed a permeable pore network for glucose, thus substantiating its suitability for the fast diffusion of nutrients.

**Keywords:** macroporous cellulose, scaffolds, lyophilization, bone tissue engineering

### INTRODUCTION

The development of polymer based three-dimensional scaffolds, which may solve clinical problems related to the loss of bone tissue, is one of the current challenges in bone tissue engineering. In this respect, natural polymers have attracted an increased interest for the preparation of bone scaffolds due to their surface chemistry, biocompatibility, non-toxicity, controllable biodegradability and mechanical strength.<sup>1</sup> Significant attention is focused on cellulose. It contains almost all properties mentioned above. However, a disadvantage of natural cellulose is its morphology, which does not correspond to the requirements for bone scaffolds as it has to be highly porous with interconnected pores – similar to the natural spongy bone tissue. The structure of the scaffolds

should be accessible for cell adhesion, proliferation, differentiation and vascularization.<sup>2,3</sup> A permeable pore network is also required for the exchange of nutrients and waste from bone cells.<sup>4</sup>

There are many studies reporting on a variety of techniques for the fabrication of desired structures, including freeze-drying,<sup>5</sup> solvent casting/particulate leaching,<sup>6</sup> electrospinning,<sup>7-9</sup> gas foaming,<sup>10,11</sup> phase separation,<sup>12</sup> rapid prototyping (stereolithography, selective laser sintering, fused deposition modelling, three-dimensional printing)<sup>13-15</sup> or even their combinations.<sup>16,17</sup>

The freeze-drying technique is widely used for producing scaffolds for tissue engineering applications.<sup>5,18-24</sup>

The method is based on the drying of pre-frozen wet samples by the means of ice sublimation in vacuum. The ice crystals formed during freezing leave holes in the structure, when the sample is dried. Using this methodology, Li *et al.*<sup>25</sup> made a biodegradable porous scaffold from chitosan and alginate with a pore size around 100-300  $\mu\text{m}$ . The interaction of osteoblasts with the scaffold confirmed its suitable structure. The scaffold promoted rapid vascularization, a connective tissue and a calcified matrix within the entire scaffold structure. A novel composite scaffold of carboxymethyl cellulose, chitosan and nano-hydroxyapatite with a great potential to be used as a bone tissue engineering material was achieved by the freeze-drying method as described by Liyun and co-workers.<sup>26</sup> Seol *et al.*<sup>27</sup> also used freeze-drying for the fabrication of chitosan sponges for bone formation. The sponges contained pores with 100-200  $\mu\text{m}$  diameter which allowed cell proliferation and bone formation. Haugh *et al.*<sup>28</sup> prepared collagen-glycosaminoglycan (CG) scaffolds. The prepared CG suspension, which contained 0.5% (w/v) collagen and 0.044% (w/v) chondroitin-6-sulfate, was degassed and lyophilized. By changing the freezing temperature, it was possible to fabricate CG scaffolds with pore sizes from 85 to 325  $\mu\text{m}$ . The results allow the hypothesis that a fast freezing process produces small crystals resulting in small pores, while the slow freezing process produces large crystals and accordingly large pores. While the rate of freezing determines the pore size, the temperature gradient across the sample determines the homogeneity of the structure. Davidenko *et al.*<sup>19</sup> found out that it was possible to create scaffolds with a multi-directional pore alignment by combining the freeze-drying with the moulding technology. The researchers prepared collagen sponge-like scaffolds with differently oriented pore channels, which depended on freezing directions.

The effect of the freezing temperature (freezing rate) on scaffold morphology was analyzed in detail.<sup>28,29-31</sup> However, there is a lack of discussion about the effect of solvent on the pore size prior to freeze-drying. Since different solvents can influence the crystallization of water, the pores appearing in the forming matrix are closely connected to this issue. In order to optimize the architecture of the scaffold, the

effect of the solvent on the porous structure of the polymeric system should be studied.

The present study aims to prepare a three-dimensional matrix of regenerated cellulose for bone tissue engineering using the freeze-drying method and to study the effect of solvent in the discontinuous phase of the gel on the morphology of the scaffold.

## EXPERIMENTAL

### Preparation of the matrix based on regenerated cellulose

A regenerated cellulose gel was prepared by the regeneration of cellulose from cellulose acetate (Sigma-Aldrich Company, degree of substitution 2.4).<sup>32</sup> The shaped gel samples of a cylindrical form with a diameter of about 18 mm and height of 40 mm were washed thoroughly with water and afterwards with the ethanol-water solution (the ethanol concentration ranged from 0 to 40% by volume). The samples were frozen at -25 °C or -80 °C and then lyophilized in a Christ ALPHA 2-4 LSC freeze-dryer (Martin Christ Gefriertrocknungsanlagen GmbH, Germany).

### Contraction of the gel

The contraction of the cellulose gel was determined by measuring volume changes after the gel samples were immersed in the ethanol-water solutions (the ethanol concentration ranged from 0 to 40%), as well as after the samples were lyophilized. The sample with a volume of 4  $\text{cm}^3$  ( $V_0$ ) was immersed in 20 mL of each solution and placed into an ultrasonic bath for 10 minutes to ensure transition of the solution into the matrix pores. After that, the sample was stored in the renewed solution at 37 °C for 24 h. The dimensions of the gel, diameter ( $d$ ) and height ( $h$ ), were measured using a Vernier calliper after the gel was taken out from the solution, as well as after lyophilization. The volume ( $V_1$ ) of the gel was calculated using Eq. (1):

$$V_1(\text{cm}^3) = \pi \times \left( \frac{d^2}{4} \right) \times h \quad (1)$$

Gel contraction ( $\Delta V$ ) was then defined by Eq. (2):

$$\Delta V (\%) = \frac{(V_0 - V_1)}{V_0} \times 100 \quad (2)$$

The experiments were repeated in triplicate and the average value was calculated.

### Morphological and structural characterization of the matrix

The morphology of the matrix and the approximate size of the pores were measured with a high resolution field emission scanning electron microscope Quanta 200 FEG (FEI Company, Netherlands) containing a Schottky type electron gun.

A magnification of 100x was used for the micrographs.

The micro-computed tomography (micro-CT) analysis was performed using a  $\mu$ CT40 micro-CT system (Scanco Medical AG, Switzerland). For the analysis, a digital cylinder with a diameter of 1000 voxels and a height of 800 voxels was extracted. The scanning settings were as follows: the scanning medium – air; the energy – 45 kV; the integration time – 600 ms; the frame averaging – 2x; the nominal resolution – 10  $\mu$ m. The data were filtered using a constrained 3D Gaussian filter to partially suppress the noise in the images ( $\sigma=0.8$ , support=1).

### Water retention

The water retained by the prepared matrices was determined using a phosphate buffer solution (pH 7.4) in order to simulate physiological conditions. The lyophilized sample, approx. 1 g ( $W_1$ ), was immersed in a solution at 37 °C for 24 h. Before weighing, the bottle with the sample was placed into an ultrasonic bath for 10 minutes to ensure that all the pores were filled with the solution. Lastly, the sample was wiped with a filter paper and weighed ( $W_2$ ). Water retention ( $WR$ ) was then defined by Eq. (3):

$$WR(\%) = \frac{W_2 - W_1}{W_1} \times 100 \quad (3)$$

### Glucose diffusion

A “side-by-side” cell (Fig. 1) was chosen for glucose diffusion within the cellulose matrix. A chamber (A) was filled with 10 mL ( $V_1$ ) of water, while the other one (B) with the same volume of 2 mmol L<sup>-1</sup> glucose solution (D-(+)-glucose, Sigma-Aldrich Company). It should be noted that the water and the glucose solution were added simultaneously to the chambers. A sample of the matrix with a diameter of 10 mm and the thickness of 1.5 mm was placed between these two chambers. The temperature was kept at 37 °C by circulating water from the thermostat. The amount of diffused glucose was determined

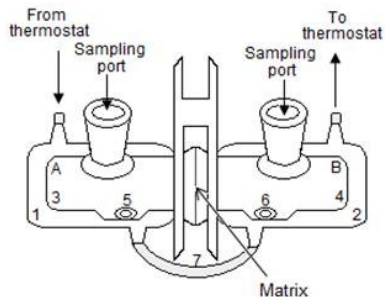


Figure 1: A “side-by-side” cell: 1, 2 – walls of chambers filled with water; 3, 4 – water and glucose solution in the chambers respectively; 5, 6 – stir bars; 7 – silicone tubing

spectrophotometrically (Varian Cary 50 UV-VIS) according to the phenol-sulfuric acid method.<sup>33</sup>

## RESULTS AND DISCUSSION

### Preparation of the cellulose-based matrix

A homogeneous semi-rigid gel was prepared by saponification of cellulose acetate in solution. As determined by the gel-inversion chromatography, its pores were accessible to molecules of a molecular mass of approx. 500000 Da. However, the pores were too small for the formation of bone tissue and nutrient transportation. The studies were focused on lyophilization of the gel in order to create a suitable morphology for bone tissue growth. Before freeze-drying, the samples were washed with ethanol-water solutions of different concentrations ranging from 0 to 40%. It was noticed that the gel changed its volume depending on the ethanol concentration. When the gel was in the water, it swelled. However, when ethanol was added into the system, the affinity of the hydrophilic polymer to the solvent decreased, which caused a structural collapse with an increased density of the polymer network. The greater the contraction, the denser was the matrix obtained (Fig. 2). After washing with 40% of ethanol, the contraction of the gel was around 12%.

The gel samples impregnated with water or water-ethanol solutions were frozen at different temperatures (-25°C or -80°C) and lyophilized in order to remove the frozen solvent, leaving a sponge with pores.

The solvent was frozen at different temperatures in order to investigate the freezing rate effect on the morphology of the scaffolds.

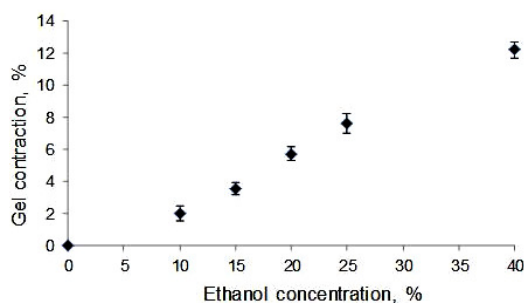


Figure 2: Dependence of gel contraction on ethanol concentration prior to freezing

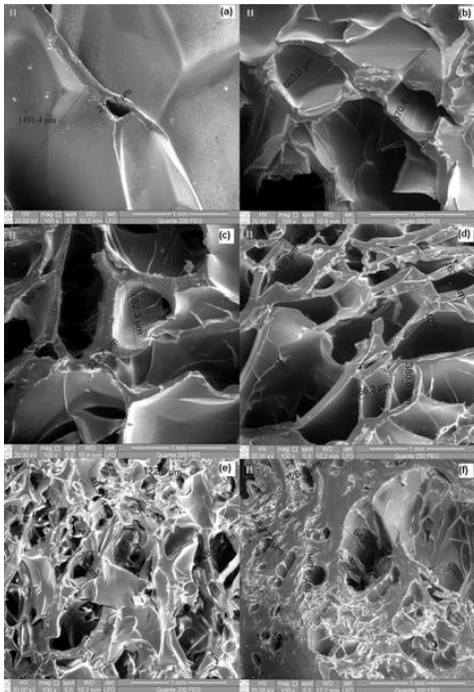


Figure 3: SEM photographs of lyophilized cellulose matrix from: (a) water; (b) 10% ethanol; (c) 15% ethanol; (d) 20% ethanol; (e) 25% ethanol; (f) 40% ethanol. \* The samples were pre-frozen at -25 °C

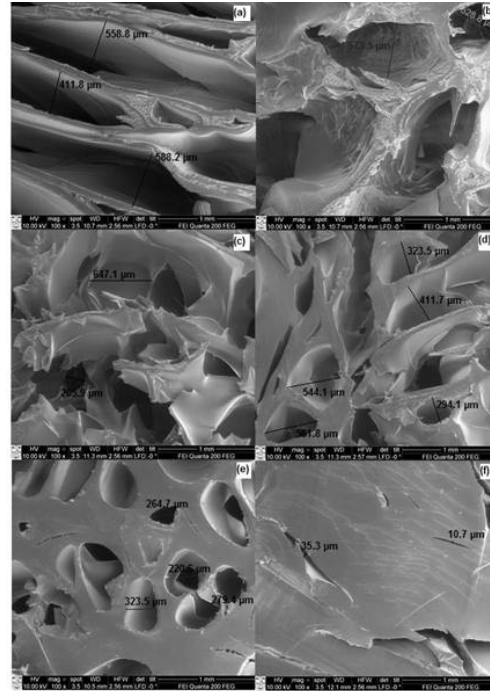


Figure 4: SEM photographs of lyophilized cellulose matrix from: (a) water; (b) 10% ethanol; (c) 15% ethanol; (d) 20% ethanol; (e) 25% ethanol; (f) 40% ethanol. \*\* The samples were pre-frozen at -80 °C

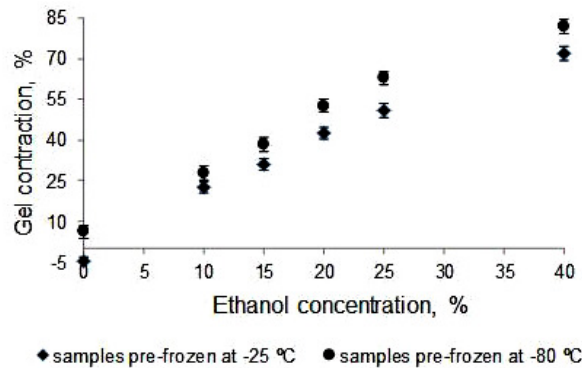


Figure 5: Dependence of gel contraction on ethanol concentration after freeze-drying

The photographs acquired by scanning electron microscopy (SEM) reveal that the morphology of the obtained scaffolds varies from a macroporous to a dense structure (Fig. 3 and Fig. 4).

It was found that such differences in the morphology of the polymer matrix were affected by the solvent inside the gel prior to lyophilization. As the drying process allows removing the solvent from the solid phase, the

samples of the gel filled with water or water-ethanol solutions were first frozen.

As demonstrated by the SEM photograph (Fig. 3a), the expanded frozen water destroyed the structure of the gel after it was filled with water, frozen at -25 °C and lyophilized. The obtained matrix was expanded for about 5% (Fig. 5). The majority of the pores were larger than 1500 μm (Fig. 3a). This kind of matrix would be unsuitable for bone scaffolds

because very large pores decrease the surface area and limit cell attachment.

The use of 10% or 15% ethanol solution slightly shrank the gel (Fig. 5), thus the matrix contained pores still rather large in diameter (Fig. 3b, c). The ideal morphology for the growth of bone tissue was obtained by filling the cellulose gel with 20% ethanol solution before its freeze-drying. The pore size ranged from micro to macro scale (Fig. 3d). The SEM images showed that the pores were distributed through the matrix homogeneously. The lyophilization of gels with 25% or 40% solutions of ethanol gave contrary results (Fig. 3e, f).

Figure 4 demonstrates the morphology of scaffolds obtained by lyophilization of the samples pre-frozen at  $-80^{\circ}\text{C}$ . Comparing the SEM photographs (Fig. 3 and Fig. 4), it can be assumed that faster freezing (at lower temperature) results in smaller pores, as it was reported by other authors.<sup>28,31</sup> In our case, faster freezing is inexpedient as clearly large or very small pores are formed (Fig. 4a, b, c, d, e). The lyophilization of the gel from 40% of ethanol gave an almost non-porous matrix (Fig. 4f).

Moreover, the SEM photographs (Fig. 4) demonstrate that not only the pore size, but also the pore form is influenced by the solvent inside the gel. When increasing the concentration of the ethanol, the pores changed from an oblong form to a spherical one.

The morphology of the scaffold, i.e., porosity, homogeneity of the porous structure and the pore size, is particularly important for cellular activity and for achieving the optimum rate of the new tissue growth. Besides, there is still a discussion about the optimal pore size

required for successful bone regeneration. According to Karageorgiou *et al.*,<sup>34</sup> a minimum pore size of  $100\ \mu\text{m}$  is required for osteogenesis as smaller pores can cause osteochondral formation. However, pore sizes greater than  $350\ \mu\text{m}$  are recommended for fast formation of vascular tissue and bone tissue.<sup>35</sup> Pisanti *et al.*<sup>36</sup> have studied the proliferation and differentiation of mesenchymal stem cells cultured under different conditions on poly-L-lactic acid scaffolds with different pore sizes of  $100$ ,  $250$  and  $500\ \mu\text{m}$ . The obtained results indicated that the cells were able to attach and maintain viability on all scaffolds with higher proliferation in the  $250\ \mu\text{m}$  and  $500\ \mu\text{m}$  pore sizes of bioreactor cultured scaffolds and  $100\ \mu\text{m}$  pore size of statically cultured scaffolds. Several authors showed that larger pore size ( $500\ \mu\text{m}$  and above) increased cell proliferation due to increasing nutrient transport throughout the scaffold, as supposed.<sup>37,38</sup>

#### **Characterization of the scaffold obtained by lyophilization from 20% ethanol solution pre-frozen at $-25^{\circ}\text{C}$**

##### ***Micro-computed tomography analysis for the morphological characterization of porous cellulose matrix***

For further morphological characterization of the prepared cellulose matrix, a micro-computed tomography (micro-CT) was chosen. Fig. 6 shows two-dimensional (2D) and three-dimensional (3D) images of the cellulose matrix.

Micro-CT images reveal interconnected porous structures. Table 1 gives the summary of the structural parameters of the regenerated cellulose matrix.

Table 1  
Structural parameters

Characteristics	Value	Unit
Total volume	625	$\text{mm}^3$
Scaffold volume	156	$\text{mm}^3$
Pore volume	470	$\text{mm}^3$
Porosity	75	%
Mean scaffold thickness	0.212	mm
Mean pore diameter	0.749	mm

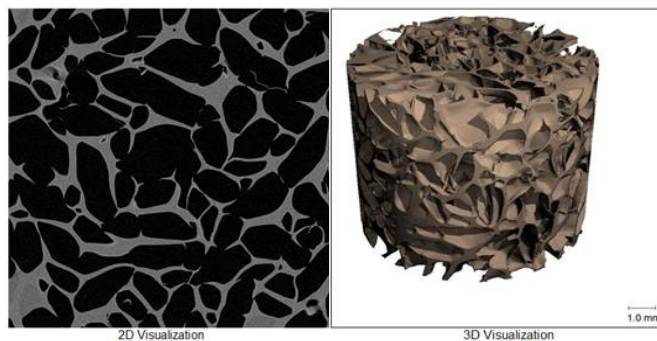


Figure 6: 2D and 3D micro-CT images of the cellulose matrix

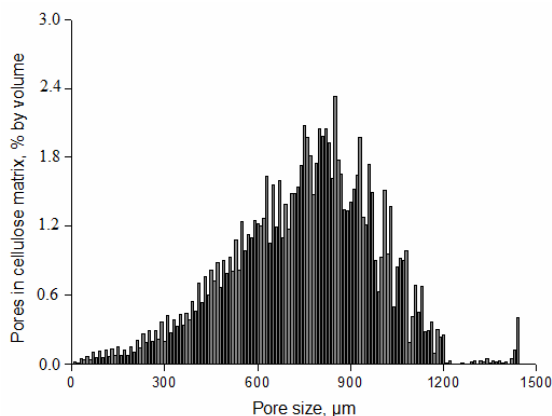


Figure 7: Pore size distribution within the cellulose scaffold

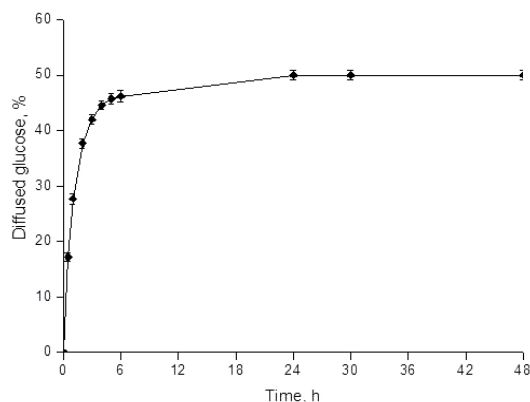


Figure 8: Glucose diffusion through the cellulose matrix

The micro-CT data indicate that the porosity of the scaffold is sufficient, since a native trabecular bone has a porosity of 50% up to 95%. The mean framework thickness is comparable to that of trabeculae of natural bone (approx. 200  $\mu\text{m}$ ).<sup>39</sup> The mean pore diameter is also in the desired range, as a natural cancellous bone has pores of up to 1 mm.<sup>40</sup>

A histogram of the pore size distribution within the cellulose scaffold is given in Fig. 7. The histogram reveals that the prepared matrix is composed of pores with different sizes. The majority of pores were from 600 to 900  $\mu\text{m}$  in size (48% of all pores). Pores from 10 to 300  $\mu\text{m}$  constituted only 4%. Pores in the range of 300-600  $\mu\text{m}$  and 900-1200  $\mu\text{m}$  represented 25 and 22%, respectively. Only 1% of pores were greater than 1200  $\mu\text{m}$ . Pores larger than 1500  $\mu\text{m}$  were not observed.

### **Hydrophilicity**

The water retention experiment showed that the prepared matrix could absorb large quantities of water; more than 5 g per 1 g of the dried

sample. This property substantiates high hydrophilicity of the matrix, which reveals biocompatibility with biological systems. The literature<sup>41</sup> indicates that the more hydrophilic a material is, the more cells adhere to the surface.

### **Nutrient transport**

The morphology of the scaffold should be appropriate for the diffusion of nutrients, otherwise necrotic regions within the material could appear. In order to substantiate the excellent morphology of the regenerated cellulose matrix for the bone scaffold, glucose diffusion through the 1.5 mm of the scaffold layer was evaluated using a side-by-side cell. Fig. 8 shows the diffused glucose within the cellulose matrix over time.

The experiment was continued until glucose concentration reached an equilibrium in both chambers. During the first four hours, the diffusion of glucose through the scaffold was very fast and the amount of diffused glucose reached up to 45%. After 6 hours, the concentration of glucose was approximately

equal in both chambers, revealing that the structure of the cellulose matrix was suitable for the transport of nutrients.

It should be noted that the diffusion of nutrients within polymer based scaffolds is different from that through ceramic scaffolds, as polymers usually absorb the solutes and release them slowly. In consequence, the rate of diffusion is affected by the morphology of the frameworks.

Our findings agree with the results reported by other researchers,<sup>42,43</sup> in particular that a high rate of nutrient diffusion is associated with high porosity and interconnected pore network of the scaffold.

## CONCLUSION

Gel morphology suitable for bone tissue engineering was successfully created by subjecting the regenerated cellulose gel to lyophilization. It was found that the porous structure of the gel depended on the solution used in its discontinuous phase before freeze-drying. By changing the concentration of ethanol in the discontinuous phase, the morphology of the lyophilized matrix could be varied from macroporous to dense. An optimal structure of the matrix was obtained by the lyophilization of the cellulose gel filled with 20% ethanol and frozen at -25 °C. The pore size of the matrix ranged from micro to macro scale, thus ensuring cell adhesion, proliferation and space for vascularization. Furthermore, the glucose transport experiment revealed the suitability of the cellulose matrix for fast diffusion of nutrients.

**ACKNOWLEDGMENT:** The work was supported by grant MIP-019/2014 from the Research Council of Lithuania.

## REFERENCES

- <sup>1</sup> D. Puppi, F. Chiellini, A. M. Piras, E. Chiellini, *Prog. Polym. Sci.*, **35**, 409 (2010).
- <sup>2</sup> J. R. Porter, T. T. Ruckh, K. C. Papat, *Biotechnol. Progr.*, **25**, 1540 (2009).
- <sup>3</sup> N. Sultana, M. Wang, *J. Mater. Sci.-Mater. M.*, **19**, 2556 (2008).
- <sup>4</sup> J. Reignier, M. A. Huneault, *Polymer*, **47**, 4703 (2006).
- <sup>5</sup> T. Lu, Y. Li, T. Chen, *Int. J. Nanomed.*, **8**, 340 (2013).
- <sup>6</sup> A. G. Mikos, A. J. Thorsen, L. A. Czerwonka, Y. Bao, R. Langer, *Polymer*, **35**, 1070 (1994).

- <sup>7</sup> A. Espindola-Gonzalez, A. L. Martinez-Hernandez, F. Fernandez-Escobar, V. M. Castano, W. Brostow *et al.*, *Int. J. Mol. Sci.*, **12**, 1910 (2011).
- <sup>8</sup> M. Ignatova, N. Rashkov, *Eur. Polym. J.*, **43**, 1114 (2007).
- <sup>9</sup> K. Rodriguez, P. Gatenholm, S. Rennecker, *Cellulose*, **19**, 1585 (2012).
- <sup>10</sup> K. Chatterjee, A. M. Kraigsley, D. Bolikal, J. Kohn, C. G. Simon Jr., *J. Func. Biomater.*, **3**, 173 (2012).
- <sup>11</sup> L. D. Harris, B. S. Kim, D. J. Mooney, *J. Biomed. Mater. Res.*, **42**, 397 (1998).
- <sup>12</sup> J. J. Blaker, J. C. Knowles, R. M. Day, *Acta Biomater.*, **4**, 266 (2008).
- <sup>13</sup> R. Landers, A. Pfister, U. Hübner, H. John, R. Schmelzeisen *et al.*, *J. Mater. Sci.*, **37**, 3110 (2002).
- <sup>14</sup> J. M. Williams, A. Adewunmi, R. M. Schek, C. L. Flanagan, P. H. Krebsbach *et al.*, *Biomaterials*, **26**, 4819 (2005).
- <sup>15</sup> I. Zein, D. W. Hutmacher, K. C. Tan, S. H. Teoh, *Biomaterials*, **23**, 1170 (2002).
- <sup>16</sup> J. E. Park, M. Todo, *J. Mater. Sci.-Mater. M.*, **22**, 1172 (2011).
- <sup>17</sup> G. Vozzi, C. Flaim, A. Ahluwalia, S. Bhatia, *Biomaterials*, **24**, 2534 (2003).
- <sup>18</sup> M. D. Ariani, A. Matsuura, I. Hirata, T. Kubo, K. Kato *et al.*, *Dent. Mater. J.*, **32**, 318 (2013).
- <sup>19</sup> N. Davidenko, T. Gibb, C. Schuster, S. M. Best, J. J. Campbell *et al.*, *Acta Biomater.*, **8**, 668 (2012).
- <sup>20</sup> R. J. Kane, R. K. Roeder, *J. Mech. Behav. Biomed. Mater.*, **7**, 42 (2012).
- <sup>21</sup> N. Ninan, Y. Grohens, A. Elain, N. Kalarikkal, S. Thomas, *Eur. Polym. J.*, **49**, 2434 (2013).
- <sup>22</sup> O. Petrauskaite, P. S. Gomes, M. H. Fernandes, G. Juodzbalys, A. Stumbras *et al.*, *Biomed. Res. Int.*, **2013**, 2 (2013).
- <sup>23</sup> B. T. Reves, J. D. Bumgardner, J. A. Cole, Y. Yang, W. O. Haggard, *J. Biomed. Mater. Res. B Appl. Biomater.*, **90**, 2 (2009).
- <sup>24</sup> K. Rinki, P. K. Dutta, *J. Macromol. Sci. A Pure Appl. Chem.*, **47**, 430 (2010).
- <sup>25</sup> Z. Li, H. R. Ramay, K. D. Hauch, D. Xiao, M. Zhang, *Biomaterials*, **26**, 3920 (2005).
- <sup>26</sup> J. Liuyun, L. Yubao, X. Chengdong, *J. Biomed. Sci.*, **16**, 65 (2009).
- <sup>27</sup> Y. J. Seol, J. Y. Lee, Y. J. Park, Y. M. Lee, Young-Ku *et al.*, *Biotechnol. Lett.*, **26**, 1038 (2004).
- <sup>28</sup> M. G. Haugh, C. M. Murphy, F. J. O'Brien, *Tissue Eng. C.*, **16**, 888 (2010).
- <sup>29</sup> N. Barbani, G. D. Guerra, C. Cristallini, P. Urciuoli, R. Avvisati *et al.*, *J. Mater. Sci.-Mater. M.*, **23**, 55 (2012).
- <sup>30</sup> S. Deville, E. Saiz, A. P. Toms, *Biomaterials*, **27**, 5481 (2006).
- <sup>31</sup> F. J. O'Brien, B. A. Harley, I. V. Yannas, L. Gibson, *Biomaterials*, **25**, 1081 (2004).

- <sup>32</sup> J. Bryjak, J. Anilyte, J. Liesiene, *Carbohydr. Res.*, **342**, 1105 (2007).
- <sup>33</sup> M. Dubois, K. A. Gilles, J. K. Hamilton, P. A. Rebers, F. Smith, *Anal. Chem.*, **28**, 350 (1956).
- <sup>34</sup> V. Karageorgiou, D. Kaplan, *Biomaterials*, **26**, 5476 (2005).
- <sup>35</sup> M. C. Wake, C. W. Patrick, A. G. Mikos, *Cell Transplant.*, **3**, 340 (1994).
- <sup>36</sup> P. Pisanti, A. B. Yeatts, S. Cardea, J. P. Fisher, E. Reverchon, *J. Biomed. Mater. Res. A.*, **100A**, 2569 (2012).
- <sup>37</sup> K. Kim, A. Yeatts, D. Dean, J. P. Fisher, *Tissue Eng. B Rev.*, **16**, 525 (2010).
- <sup>38</sup> T. Mygind, M. Stiehler, A. Baatrup, H. Li, X. Zou *et al.*, *Biomaterials*, **28**, 1044 (2007).
- <sup>39</sup> M. Doblare, J. M. Garcia, M. J. Gomez, *Eng. Fract. Mech.*, **71**, 1812 (2004).
- <sup>40</sup> T. M. Keaveny, E. F. Morgan, G. L. Niebur, O. C. Yeh, *Ann. Rev. Biomed. Eng.*, **3**, 308 (2001).
- <sup>41</sup> Y. Tamada, Y. Ikada, *J. Biomed. Mater. Res.*, **27**, 19 (1994).
- <sup>42</sup> T. S. Karande, J. L. Ong, C. M. Agrawal, *Ann. Biomed. Eng.*, **32**, 1736 (2004).
- <sup>43</sup> A.G. Mitsak, J. M. Kemppainen, M.T. Harris, S.J. Hollister, *Tissue Eng. Part A.*, **17**, 1832 (2011).